



# Effect of microencapsulation phase change material and diatomite composite filling on hygrothermal performance of sintered hollow bricks



Youssef Fraine<sup>a,\*</sup>, Chakib Seladji<sup>a</sup>, Abdelkarim Aït-Mokhtar<sup>b</sup>

<sup>a</sup> *Laboratory of Energy and Thermal Applied (ETAP), University of Tlemcen, B. P 230, Tlemcen, 13000, Algeria*

<sup>b</sup> *LaSIE UMR 7356, University of La Rochelle-CNRS, Avenue M. Crépeau, 17042, La Rochelle, France*

## ARTICLE INFO

### Keywords:

Coupled heat and moisture transfer  
Sintered hollow brick  
MPCM/diatomite  
Porous media

## ABSTRACT

The aim of the present study is to investigate the use of a new phase change humidity control material (PCHCM) as a replacement for the expanded polystyrene (EPS) in hygrothermal insulation of the building construction. PCHCM is prepared by incorporating microencapsulation phase change material (MPCM) and diatomite, it is filled in a sintered hollow bricks typically used in the construction of Algerian buildings, considering different configurations, in order to get optimum insulation. A two dimensional coupled heat and moisture transfer model has been developed and solved numerically using a finite element method to study, and compare the effect of EPS, diatomite, and PCHCM on the comfort level of the building indoor environment. Different filling ratios of PCHCM and its locations are considered to reach the best hygrothermal performance. The inner temperature and relative humidity fluctuations obtained from the study are significantly reduced in comparison with EPS. In addition, the optimal location of PCHCM is given when it is filled with 66% in the internal side of the hollow brick. MPCM/diatomite composite was found to have the potential to save energy reaching 50% compared to EPS and can be used as a hygrothermal insulation material in building construction.

## 1. Introduction

Energy demand and environmental protection issues are two major challenges faced by mankind and have always been a preoccupation of the researchers all over the world [1,2]. Energy use in human societies increases quickly with the fast increase in living standards during the last two decades [3,4,5]. Energy from fossil fuels is the most commonly used in developing countries, and burning them increase greenhouse gas emissions, which leads to climate change and environmental pollution [6,7]. Therefore, it is crucial now to improve energy efficiency by reducing fossil energy consumption and tackle climate change. Related to this, building sector accounts for about 45% percent of the world's total energy consumption and responsible for 36.1 billion tons of CO<sub>2</sub> emissions. Energy consumption in the building comes mainly from heating, ventilation and air conditioning (HVAC) systems [4,7,8]. Many methods were introduced to reduce building energy consumption, through improving the efficiency of HVAC systems, and using innovative passive materials to control the indoor temperature and humidity, ensuring a good comfort level of the indoor space [6,7,9].

Temperature and relative air humidity are very important among environmental parameters affecting the quality of the indoor space. Fluctuation of ambient temperature due to the day/night and winter/

summer alternations lead to a thermal dis-comfortable in the living environment [3,7]. Some works study thermal storage in materials as PCM's to contribute to the stabilization of indoor temperature [10]. PCM's can absorb and release a large amount of energy by changing their phase from solid to liquid, and from liquid to solid at a constant temperature during the phase change process, respectively [11,12]. Integration of PCM's in building by encapsulation in structural materials has been proposed as the best method of increasing the energy efficiency of buildings, improving occupant comfort, and decreasing energy consumption [13–15].

Humidity is also fluctuant and it is related to human health problems and living environment [16,17]. An excessive change in relative humidity can affect construction durability, the storage of goods, and energy consumption [18,19]. Research studies show that maintained indoor relative humidity in the range of 30%–60% is the most comfortable living environment [20]. Humidity control materials (HCM) are a porous material that can absorb or release moisture automatically without any power source or mechanical equipment due to its sensitivity to the variations of ambient relative humidity, and ambient temperature [18,20–22]. Research dealing with the use of HCM has initially started in Japanese Institute [23]. Various HCMs were developed, including biomass HCM [24,25], inorganic HCM [18,26], and organic HCM [27,41]. Consequently, the use of an HCM is of great

\* Corresponding author.

E-mail address: [yousseuf.fraine@mail.univ-tlemcen.dz](mailto:yousseuf.fraine@mail.univ-tlemcen.dz) (Y. Fraine).

<https://doi.org/10.1016/j.buildenv.2019.02.036>

Received 30 November 2018; Received in revised form 24 February 2019; Accepted 25 February 2019

Available online 02 March 2019

0360-1323/ © 2019 Elsevier Ltd. All rights reserved.

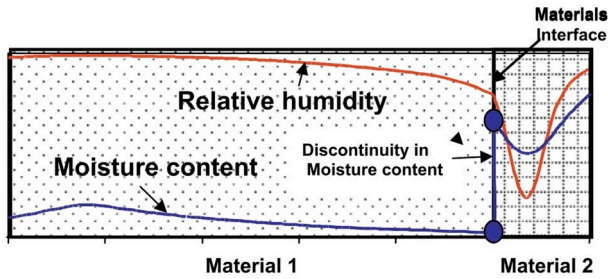


Fig. 1. Example of relative humidity and moisture content profiles at the interface of two dissimilar materials [36].

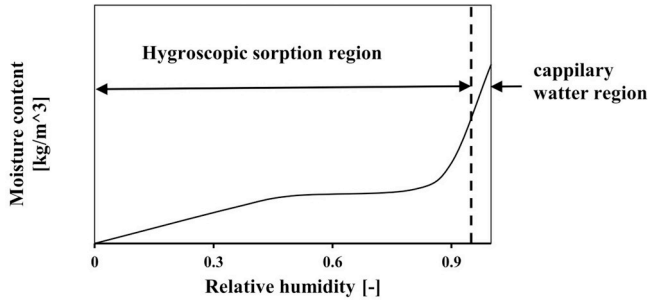


Fig. 2. Sorption isotherm of a typical material.

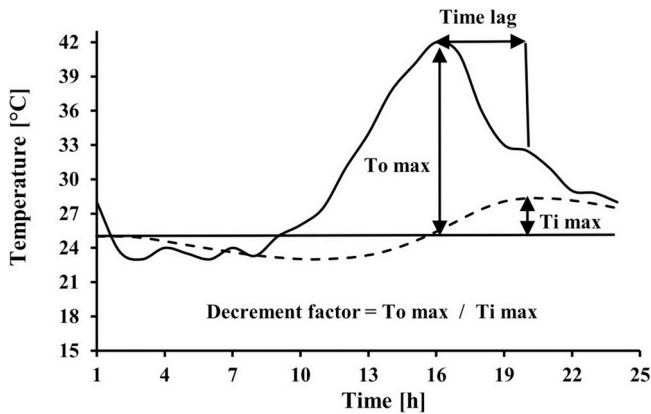


Fig. 3. A schematic definition of time lag and decrement factor for temperature.

importance to the sustainable development of ecological environment, it can adjust indoor humidity, and reduce energy demand [20,21].

Recently, several approaches have been investigated in order to optimize the hygrothermal performance of building envelope in order to develop a passive material, which could provide indoor thermal, and humid buffering capacity [28,29]. Some researchers have attempted to prepare a novel endothermal-hygroscopic material by synthesizing MPCM and porous HCM. It has the ability to control temperature and humidity of the indoor environment [4]. Yuan et al. [30], proposed the Polyethylene glycol (PEG2000) organic polymer with different water contents as endothermal-hygroscopic material. Karaman et al. [31], reported on the PEG/diatomite composite as a novel form-stable PCM's. The PEG could be retained by 50% mass into pores of the diatomite matrices without the leakage of melted PEG from the composite. Shang [32], prepared the  $Na_2SO_4 \cdot 10H_2O$ /sepiolite, paraffin/sepiolite, and dodecanol/sepiolite composites by injecting the PCM's in-to porous sepiolite. Qin et al. [6], prepared several PCHCMs using PCM microcapsules with  $SiO_2$  as a shell, and the vesuvianite, sepiolite, and zeolite as a hygroscopic material. Results indicate that the CPCM/vesuvianite composite has a better hygrothermal performance than the other two PCHCMs. Wu et al. [4], prepared MPCM/diatomite composite with 12.9% ratio of the encapsulation PCM. Chen et al. [3], prepared a

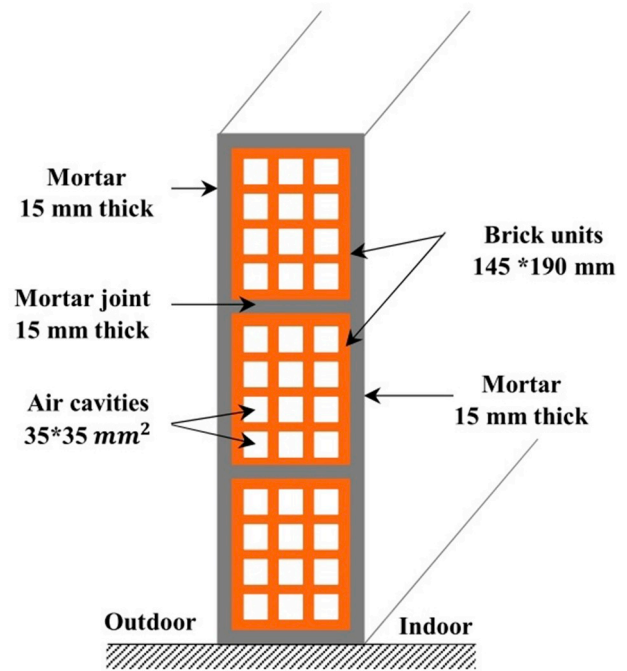


Fig. 4. Axonometric view of a typical sintered hollow bricks wall commonly used in Algeria.

PCHCM with different encapsulation mass ratios of PCM, using  $SiO_2$  as a shell and diatomite as a hygroscopic material. Results show that the shell  $SiO_2$  can reduce the super-cooling degree of PCM melts, and prevent the leakage of the PCM's. It did not affect the hygroscopic properties of the diatomite. The MPCM/diatomite composite is efficient in thermal storage and moisture adjusting. It can be used in interior wallboard of buildings [3,4].

The current paper addresses the question of substituting the EPS by using diatomite, and the optimized diatomite (MPCM/diatomite composite) in order to reduce the building energy consumption. Diatomite is highly porous, light in weight and chemically stable, and inert [46]. It has been extensively applied in many ways such as water filtration and purification, thermal insulation due to its low thermal conductivity, manufacture of antibiotics, some pharmaceutical syrups, and it is qualified as an ecological material [34,35]. While the EPS is a chemical material containing a contaminant named Hexabromocyclododecane (HBCD). The HBCD used as a brominated flame retardant in the EPS. Its toxicity and harm to the environment are currently discussed in the Stockholm Convention, and it is added to the list of Persistent Organic Pollutant (POP) in Annex A [33].

To answer this issue, a coupled heat and moisture transfer model for the building envelope is developed and benchmarked against one of the fifth HAMSTAD tests [40], and a two dimensional numerical simulations are realized using finite element method and an explicit scheme, to study the effect of EPS, diatomite, and MPCM/diatomite composite on hygrothermal performance of a fired clay sintered hollow bricks typically used in construction of Algerian buildings. The improvement of the hollow brick insulation performance is achieved by filling MPCM/diatomite composite according to different configurations, and comparing the influence of filling ratios, and locations on hygrothermal performance. The climate conditions considered are those in the northwest zone in Algeria (South-Mediterranean climate) [43].

## 2. Mathematical models

### 2.1. Coupled heat and moisture transfer equations

In the present model, we consider the temperature and the relative

humidity as driving potentials governing the heat and moisture transfer, providing the continuity of variables at the interface between the layers. The moisture content is discontinuous as illustrated in Fig. 1.

Each material has a unique equilibrium moisture content characteristic curve (sorption isotherm) that identify the moisture mechanisms transfer in pores. The moisture mechanism transfer can be by vapor diffusion in the hygroscopic region as illustrated in Fig. 2 and can be by capillary suction in the capillary water region, where the relative humidity is over 95%.

Based on the study of HM Kunzel [37], the following assumptions are considered:

- The material is considered homogeneous and non-deformable.
- The thermal equilibrium between all phases is assumed.
- The dry air and the water vapor are ideal gas and non-compressible.
- Chemical reactions and the hysteresis effect are not considered.
- The effect of gravity on the fluid flow is not taken into account.

The general form of the governing equations describing heat and moisture transfer processes in porous materials are given by a system of two partial differential equations derived by imposing the equilibrium balance of mass and energy within an infinitesimal element of volume [37]:

$$\rho_s \left( c_s + \frac{1}{\rho_s} c_w w \right) \frac{\partial T}{\partial t} = \nabla \left[ \left( \lambda + h_v \delta_p \varphi \frac{\partial P_{sat}}{\partial T} \right) \nabla T + h_v \delta_p P_{sat} \nabla \varphi \right] \quad (1)$$

$$\xi \frac{\partial \varphi}{\partial t} = \nabla \left[ \delta_p \nabla \varphi \frac{\partial P_{sat}}{\partial T} \nabla T + (D_w \xi + \delta_p P_{sat}) \nabla \varphi \right] \quad (2)$$

Where,  $\rho_s$  is the bulk density of the dry building material in  $[kg/m^3]$ ;  $c_s$  the specific heat capacity of dry building material in  $[J/(kg. K)]$ ;  $c_w$  the specific heat capacity of water in  $[J/(kg. K)]$ ;  $w$  Water content in  $[kg/m^3]$ ;  $T$  temperature in  $[K]$ ;  $\lambda$  thermal conductivity in  $[W/(m. K)]$ ;  $h_v$  evaporation enthalpy of water in  $[J/kg]$ ;  $\delta_p$  water vapor permeability of the building material in  $[kg/(m. s. Pa)]$ ;  $\varphi$  Relative humidity;  $P_{sat}$  Water vapor saturation pressure in  $[Pa]$ ;  $\xi$  Moisture storage capacity in  $[kg/m^3]$ ;  $D_w$  Moisture diffusion coefficient  $[m^2/s]$ .

The MPCM/diatomite composite was modeled using the coupled heat and moisture transfer model presented above. The PCM was incorporated into the porosity of the diatomite. The volume fraction of diatomite was defined as  $\theta_d$ , and thus the volume fraction of PCM was equal to  $(1 - \theta_d)$ .

Therefore, the effective thermal properties of the media assuming a parallel configuration are:

$$(\rho cp)_{eff} = \rho_d cp_d \theta_d + \rho_{pcm} cp_{pcm} (1 - \theta_d) \quad (3)$$

The PCM was modeled using modified specific heat capacity:

$$cp_{pcm} \begin{cases} P_s & \text{if } T_m < T \\ \left( \frac{cp_s + cp_l}{2} + \frac{L - hv}{\Delta T} \right) & \text{if } T_m \leq T \leq (T_m + 1) \\ cp_l & \text{if } T > (T_m + 1) \end{cases} \quad (4)$$

Where, the subscript d stands for diatomite,  $cp_l [J/(kg. K)]$  is the specific heat capacity of PCM in liquid form, and  $cp_s [J/(kg. K)]$  is the specific heat capacity of PCM in solid form.

The Moisture boundary conditions for exterior and interior surfaces of the building wall are taken by Eqs. (5) and (6), respectively:

$$\delta_p \nabla \varphi \frac{\partial P_{sat}}{\partial T} \nabla T + (D_w \xi + \delta_p P_{sat}) \nabla \varphi = \beta_{ext} (\phi_{ext} P_{sat}(T_{ext}) - \varphi P_{sat}(T)) \quad (5)$$

$$\delta_p \nabla \varphi \frac{\partial P_{sat}}{\partial T} \nabla T + (D_w \xi + \delta_p P_{sat}) \nabla \varphi = \beta_{int} (\phi_{int} P_{sat}(T_{int}) - \varphi P_{sat}(T)) \quad (6)$$

Where,  $\beta_{ext}$  and  $\beta_{int} [s/m]$  are the vapor transfer coefficient at the wall

surfaces,  $P_{sat}(T)$  Water vapor saturation pressure as a function of temperature in  $\varphi$  Relative humidity,  $\phi_{int}$  and  $\phi_{ext}$  are the relative humidity in the interior and exterior of the wall, respectively.

While Eqs. (7) and (8) give the heat flow boundary conditions at the exterior and the interior surfaces of the building wall. In these equations both heat convection and radiation are taken into accounts:

On the outside of the wall:

$$k_{eff} \nabla T + h_v \delta_p P_{sat} \nabla \varphi = h_{ext} (T_{ext} - T) + \varepsilon \sigma (T_{\infty}^4 - T_{ext}^4) + \beta_{ext} h_v (\phi_{ext} P_{sat}(T_{ext}) - \varphi P_{sat}(T)) \quad (7)$$

On the inside of the wall:

$$k_{eff} \nabla T + h_v \delta_p P_{sat} \nabla \varphi = h_{int} (T_{int} - T) + \beta_{int} h_v (\phi_{int} P_{sat}(T_{int}) - \varphi P_{sat}(T)) \quad (8)$$

Where  $\varepsilon$  is the long wave emissivity and absorptivity of the material,  $\sigma$  the Stefan-Boltzman constant in  $[W/(m^2. K^4)]$ ,  $T_{\infty}$  the sky temperature  $h_{ext}$ , and  $h_{int}$  are exterior and interior heat transfer coefficients for air wind, respectively.

The convective heat transfer coefficient for air wind, interior air, and the sky temperature can be found in Ref. [38] as:

$$h_{int} = 2.8 + 3v_a \quad (9)$$

$$h_{ext} = 2.8 + 3v_{wind} \quad (10)$$

$$T_{\infty} = 0.0552(T_a)^{1.5} \quad (11)$$

Where  $v_a$  is the average interior air, it is taken equal to  $0.15 [m/s]$ , according to ASHRAE standards as comfortable ventilation velocity [39], and  $v_{wind}$  is the wind velocity, taken as function of time:  $v_{wind}(t) [m/s]$ .

## 2.2. Time lag and decrement factor

Time lag and decrement factor are required characteristics to determine heat and moisture storage capabilities of any material. As mentioned in the work of Asan [45], due to the periodic changes of outside temperature during the 1-day period, temperature profiles are variables during the day. The time it takes for the heat wave to propagate from the outer surface to the inner surface is named “time lag”, and the reduction in the cyclical temperature (amplitude) on the inside surface compared to the outside surface is known as “decrement factor”. The same definition can be used to define time lag and decrement factor of relative humidity. A schematic definition of time lag and decrement factor for temperature are shown in Fig. 3.

In this study, the time lag is described as follows:

$$Time\ lag = \begin{cases} t_{T_o}^{max} > t_{T_i}^{max} \Rightarrow t_{T_o}^{max} - t_{T_i}^{max} \\ t_{T_o}^{max} < t_{T_i}^{max} \Rightarrow t_{T_o}^{max} - t_{T_i}^{max} + P \\ t_{T_o}^{max} = t_{T_i}^{max} \Rightarrow P \end{cases} \quad (12)$$

Where  $t_{T_o}^{max} [h]$  and  $t_{T_i}^{max} [h]$  represent the time in hours when outside and inside surface temperatures and relative humidity are at their maximums, respectively and P (24 h) is the period of the wave. The decrement factor is described as follows:

$$Decrement\ factor = \frac{y_o^{max} - y_o^{min}}{y_i^{max} - y_i^{min}} \quad (13)$$

Where  $y_o^{max}$ ,  $y_i^{max}$ ,  $y_o^{min}$  and  $y_i^{min}$  represent the outside and the inside surface temperature and relative humidity at their maximums, and minimums, respectively.

**Table 1**  
Hygrothermal properties of used materials.

Properties	Diatomite [21,41]	Air [2]	Brick [2]	Mortar [2]	EPS [44]	PCM (100%) [4]		PCHCM (12.9%PCM) [4]	
						liquid	Solid	liquid	Solid
$\rho_s$ [kg/m <sup>3</sup> ]	666.7	1.23	1600	230	20	775	814	680.67	685.7
cp [J/kg K]	1436	1006.43	840	920	1500	2660	2140	1615.8	1543.8
$\lambda$ [W/m K]	0.7	0.026	0.682	0.6	0.04	0.149	0.35	0.62	0.65
$\delta \times 10^{-10}$ [kg/m s Pa]	0.295	5.62	0.26	0.0385	0.0187	–	–	5	–
Melting Temp [°C]	–	–	–	–	–	28.1	–	27.0	–
Latent heat [kJ/kg]	–	–	–	–	–	145.9	–	19	–

**3. Description of the physical model**

To improve the construction mode in Algeria, the insulation materials could be included in the cavities of a sintered hollow bricks wall, which may well suppress the moisture and heat transfer. The coupled heat and moisture transfer model presented is used to investigate the impact of different hygroscopic materials on the hygrothermal performance of a typical exterior wall of the residential building in Algeria.

The configuration of the typical sintered hollow bricks wall commonly used in the construction of the residential building in Algeria is presented in Fig. 4. The exterior wall is built of:

- A sintered hollow bricks of a big size with 12 equal air cavities (BB12CE), and a weight of 5–6 kg. Its dimensions are 30 cm in length, 19 cm in width and 14.5 cm in thickness. The air cavities have a parallelepiped section ( $3.5 \times 3.5 \text{ cm}^2$ ).
- A cement based mortar with a ratio of 1/3 cement to sand is used in both joint, and in the two sides (interior and exterior surfaces) of the wall with a thickness of 1.5 cm.
- EPS, diatomite, and PCHCM are filled in bricks cavities as insulation materials in order to compare its effect on the hygrothermal performance of the sintered hollow bricks.

The hygrothermal properties of used materials are listed in Table 1 and shown in Fig. 5.

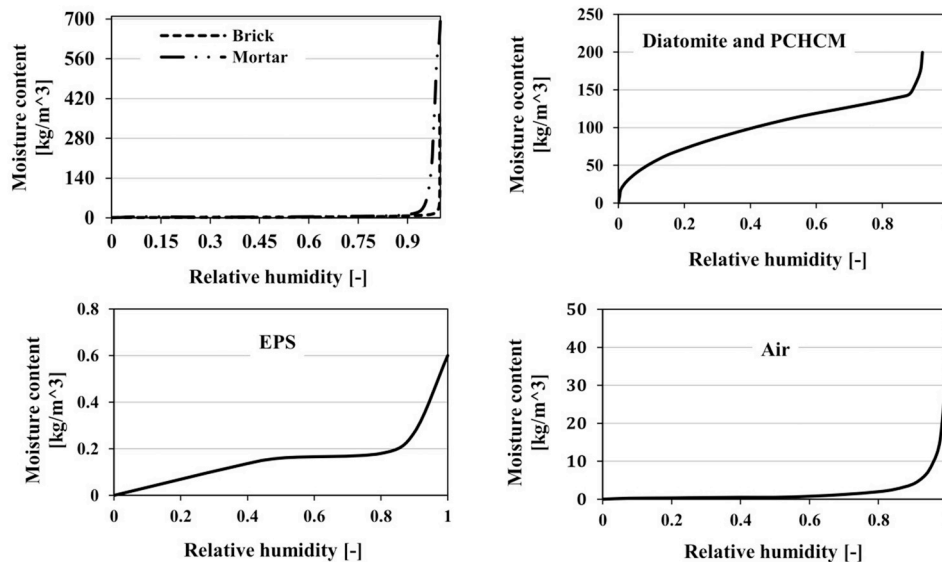


Fig. 5. Sorption isotherms of the materials constituting the studied cases according to Refs. [21,44].

As shown in Table 1, the PCM encapsulation ratio has a great effect on the amount of energy released or absorbed during the change of the PCM and PCHCM. In addition, the lack of heat absorption process of diatomite contributes to the worst heat storage capacity of PCHCM.

Due to the symmetry of the geometry and boundary conditions in the longitudinal direction of the wall (Z direction), the problem is addressed in two dimension. The outdoor surface of the wall is simultaneously subjected to a time-dependent temperature ( $T_{ext}(t)$ ), relative humidity ( $\varphi_{ext}(t)$ ), solar radiation with absorptivity  $\varepsilon = 0.87$  [2], and forced convection  $h_{ext} = 2.8 + 3v_{wind}$  [38]. The related outdoor time-dependent variables (air temperature, air relative humidity, solar radiation) considered in this study (Fig. 6) are taken from typical meteorological daily data of Tlemcen region in the northwest of Algeria (the hottest day in 07 August 2017) [43].

On the indoor surface of the wall, an imposed relative humidity  $\varphi_{int} = 50\%$ , and free convection boundary condition  $h_{int} = 3.25 [W/m^2K]$ , with the temperature of the air contacts  $T_{int} = 25 [°C]$  are chosen as the comfortable living environment condition. At the beginning, the temperature and relative humidity are respectively at  $T_{ini} = 25 [°C]$  and  $\varphi_{ini} = 50\%$ .

**4. Results and discussions**

In this section, two parts are presented. The first one is related to the validation aspect considering some benchmark tests given in the

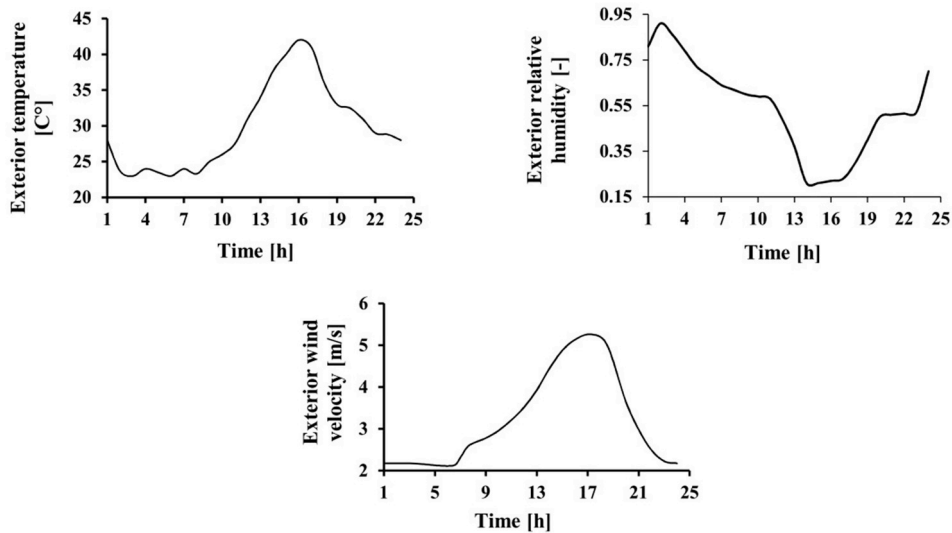


Fig. 6. Variation of outdoor temperature, relative humidity, and air velocity used in simulations [43].

literature. The second part is dedicated to the analysis of the diatomite, EPS, and MPCM/diatomite composite filling impacts on the hygro-thermal performance of the considered hollow bricks wall (case 01). In order to get optimal performance, different filling ratios and locations of PCHCM are considered (case 02), analyzed and compared. The mathematical model of coupled heat and moisture transfer represented by equations (1) and (2) is solved numerically using finite element method, and an explicit scheme with variable time stepping, based computational COMSOL Multiphysics tool [42]. By using the partial differential interface in the COMSOL program (PDE equations), we can define own coupled heat and moisture transfer model by specifying the equations parameters and driving potentials. As a results of simulations, temperature and relative humidity can be determined at any location, and can be exported as a data file, and plotted.

4.1. Model validation

The presented model is benchmarked using HAMSTAD tests [40], which were initiated to develop a platform to assess the computational modeling of heat, moisture, and air transport mechanisms in building physics.

In the benchmark test, a moisture redistribution inside a multilayers wall was analyzed in one dimension, and the properties of capillary

Table 2

Material properties definition of layers [40].

Parameters	value
Sorption isotherm [kg/m <sup>3</sup> ] as function of capillary suction $P_{suc}$ [Pa]	$w(P_{suc}) = w_{sat} \sum_{i=1}^N \frac{k_i}{(1 + (a_i h(P_{suc}))^{m_i})^{m_i}}$
Capillary suction height [m]	$h(P_{suc}) = P_{suc}/(\rho_w g)$
Kelvin relation	$P_{suc}(\phi) = -\rho_w R v T \ln(\phi)$
Vapor gas constant	$R_v = R/M_w$
The vapor diffusion [m <sup>2</sup> /s]	$D_v(w) = \frac{26.1 \cdot 10^{-6}}{RT} \frac{1 - \frac{w}{w_{sat}}}{(1-p)(1 - \frac{w}{w_{sat}})^2 + p}$
Liquid water permeability [s]	$\delta_p(w, T) = \frac{M_w}{RT} D_v(w)$
Liquid water conductivity [s]	$k(w) = \exp[\sum_{i=0}^5 a_i (w/\rho_w)^i]$
Thermal conductivity [W/m k]	$\lambda = (\lambda_{matry} + \lambda_{mst} \frac{w}{\rho_w})$
Volumetric liquid water content [m <sup>3</sup> /m <sup>3</sup> ]	$\theta_l(w) = w/\rho_w$
The reference temperature [K]	$T = 293.15$
Liquid water density [kg/m <sup>3</sup> ]	$\rho_w = 1000$
Molar water mass [kg/mol]	$M_w = 0.018$
Universal gas constant [J/mol K]	$R = 8.314$
Gravity acceleration [m/s <sup>2</sup> ]	$g = 9.81$

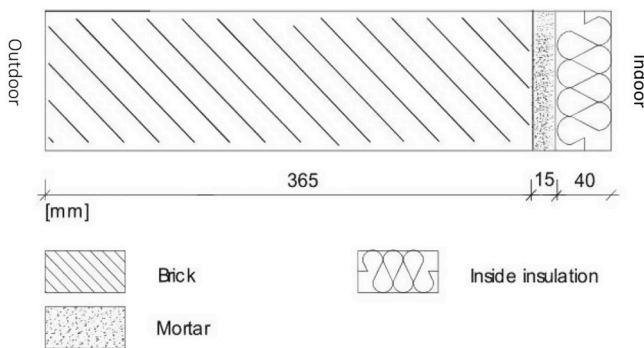


Fig. 7. An inside insulated wall structure with initial temperature and relative humidity of  $T = 25^\circ C$ .

active insulations were calculated. The wall consists of three materials from exterior to interior as shown in Fig. 7: brick (365 mm thick), coating mortar (15 mm thick), and an insulating material (40 mm thick). The structure is airtight.

$\phi = 60\%$ , and boundary conditions of  $T = 0^\circ C$ ,  $\phi = 80\%$ ,  $T = 20^\circ C$ ,  $\phi = 60\%$  at the outside and inside of the structure, respectively [40].

The simulation time is 60 days. As results of the simulation using the coupled heat and moisture transfer model, both moisture content and relative humidity at last time step (60 days) are shown in Fig. 8a and Fig. 8b, and compared with the values of benchmark solutions. The numerical solutions show a good agreement for all positions, and in Fig. 8b, a discontinuity is visible because each material has its own moisture sorption curve.

**Table 3**  
Parameters for all given materials [40].

	Brick	Mortar	Inside insulation
<i>Sorption isotherm</i>			
water saturation $w_{sat}$ [kg/m <sup>3</sup> ]	373.5	700	871
$k_1$ [-]	0.46	0.2	0.41
$k_2$ [-]	0.54	0.8	0.59
$a_1$ [-]	0.47	0.5	0.006
$a_2$ [-]	0.2	0.004	0.012
$n_1$ [-]	1.5	1.5	2.5
$n_2$ [-]	3.8	3.8	2.4
<i>Vapor diffusion [m<sup>2</sup>/s]</i>			
$p$ [-]	0.2	0.2	0.2
<i>Liquid water conductivity [s]</i>			
$a_0$ [-]	-36.484	-40.425	-46.245
$a_1$ [-]	461.325	83.319	294.506
$a_2$ [-]	-5240	-175.961	-1439
$a_3$ [-]	2.907 10 <sup>4</sup>	123.863	3249
$a_4$ [-]	-7.41 10 <sup>4</sup>	0	-3370
$a_5$ [-]	6.997 10 <sup>4</sup>	0	1305
<i>Thermal conductivity [W/m K]</i>			
Dry material $\lambda_{mdry}$	0.682	0.6	0.06
Saturation material $\lambda_{mst}$	0	0.56	0.56
<i>Heat capacity</i>			
Density [kg/m <sup>3</sup> ]	1600	230	212
Specific heat capacity [J/(kg K)]	1000	920	1000

4.2. Cases studies

Due to the symmetry of the cells in the bricks wall, one cell of the brick surrounded by mortar is taken in all simulations for the cases studies, with an insulation condition in both below, and above the brick cell as illustrated in Fig. 9.

4.2.1. Case 01

In order to improve the hygrothermal performance of the hollow bricks wall, the influence of filling diatomite, PCHCM, and EPS in cavities of the sintered hollow bricks on heat and moisture transfer are analyzed and compared.

As results, the time-variations of temperature and relative humidity at the inner surface of the bricks unit surrounded by mortar, and filled by different hygroscopic materials are shown in Fig. 10.

As shown in Fig. 10, there is an obvious difference between outside and inside temperature and relative humidity fluctuations under different hygroscopic materials. It can be clearly seen that air, and EPS can reduce the inner surface temperature, and relative humidity better than diatomite due to the difference in thermal conductivity, and hygroscopicity. Whereas, filling PCHCM in brick cavities gives the lowest fluctuation of temperature, and relative humidity compared to other materials, and the reduction of total heat flux (THFR) by using relationship (14) is 50% in 24 h compared to EPS which is 11.62% as shown in Fig. 11.

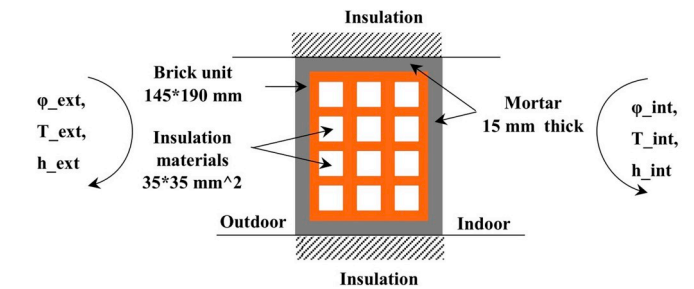
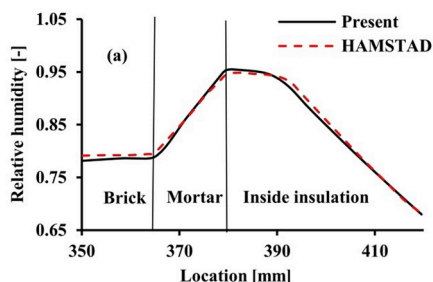


Fig. 9. A two-dimensional section of the cell of sintered hollow brick and mortar. Filled by different hygroscopic materials used in the simulation.

$$THFR (\%) = \frac{\text{total heat flux without insulation} - \text{total heat flux with insulation}}{\text{total heat flux without insulation}} * 100 \tag{14}$$

The difference in fluctuations can be explained by the fact that PCHCM contains the PCM, while the latter has the capability to absorb a large amount of energy, and needs more time to change his state from solid to liquid. This fact leads to a decrease in inner surface temperature. In addition, it contains diatomite; which can absorb water vapor due to its high porosity, leading to a decrease of inner surface relative humidity.

4.2.2. Case 02

Based to the results of the first case, the improvement of hygrothermal performance of the hollow bricks is achieved by filling the MPCM/diatomite composite in the holes of bricks.

In this part, the effect of different filling ratios of PCHCM, and its locations in sintered hollow bricks is studied and analyzed in order to obtain the best insulation (Fig. 12). All configurations are subjected to the same boundaries conditions of the case (01) in Fig. 9.

The variation of the inner surface temperature, and the relative humidity under different PCHCM filling ratios, and locations are figured in Fig. 13.

As shown in Fig. 13, under the same PCHCM filling ratio of 33% (Fig. 12), PCHCM filled in the internal air cavities has the lowest temperature, and relative humidity fluctuations (see case (B\_3)), while PCHCM filled in center, and internal air cavities simultaneously has the lowest temperature, and relative humidity fluctuations for the case (C\_2) with filling ratio of (66%). On the other hand, with the increase of PCHCM filling ratios from case (A) to case (C), the temperature, and relative humidity fluctuations decrease gradually, but when the filling ratio attain the max value (see case (D)), an increase in fluctuations of inner surface temperature and relative humidity is observed.

Variation of decrement factor of inner surface temperature, and relative humidity with different filling ratios, and locations of PCHCM are shown in Fig. 14. It can be seen that there is an inverse relationship between decrement factor, and PCHCM filling ratios. Moreover, we observe a large difference of decrement factor for the same filling ratio due to PCHCM locations. This result means that inner temperature, and

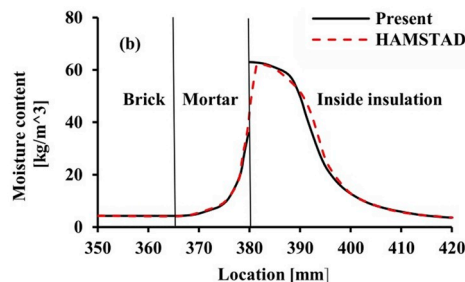


Fig. 8. Simulation results after 60 days: (a) Relative humidity [-] profile; (b) Moisture content [kg/m<sup>3</sup>] profile.

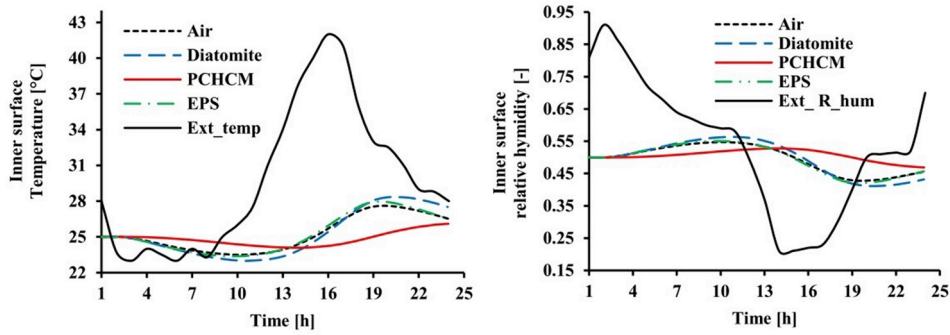


Fig. 10. Time-variation of inner temperature and relative humidity vs external conditions (Ext\_temp, Ext\_R\_him) under different hygroscopic materials filling.

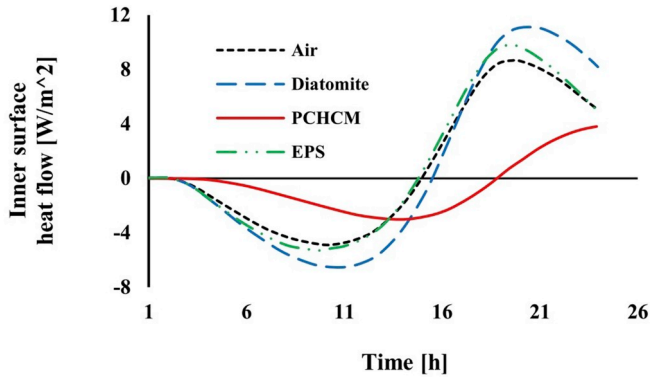


Fig. 11. Time-variation of the inner surface thermal flux under different hygroscopic materials.

relative humidity trends to stabilize, reaching a high indoor comfortable level.

Variations of time lag of inner surface temperature, and relative humidity according to different filling ratios, and locations of PCHCM are shown in Fig. 15. As indicated, there is a direct relationship between time lag and PCHCM filling ratios, and a large difference of time lag of inner temperature of the same filling ratio due to PCHCM locations.

### 5. Conclusion

The MPCM/diatomite composite has been proposed as an alternative solution for the substitution of EPS, for adjusting indoor temperature and relative humidity. The insulation material is filled in air cavities of a sintered hollow brick. The effect of filling ratios, and locations of PCHCM on hygrothermal performances of a hollow brick under Tlemcen city (the northwest of Algeria) climate conditions are analyzed using finite element methods. Results show that PCHCM has a

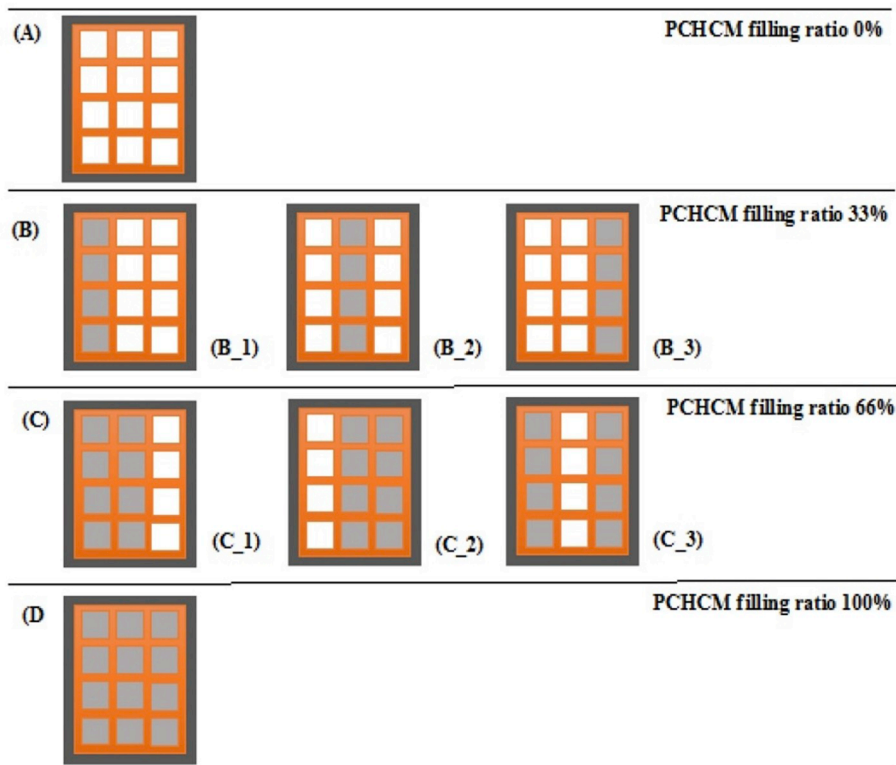


Fig. 12. Schematic diagram of the cell of sintered hollow brick surrounded by Mortar with different PCHCM filling ratios and locations, from outdoor to indoor.

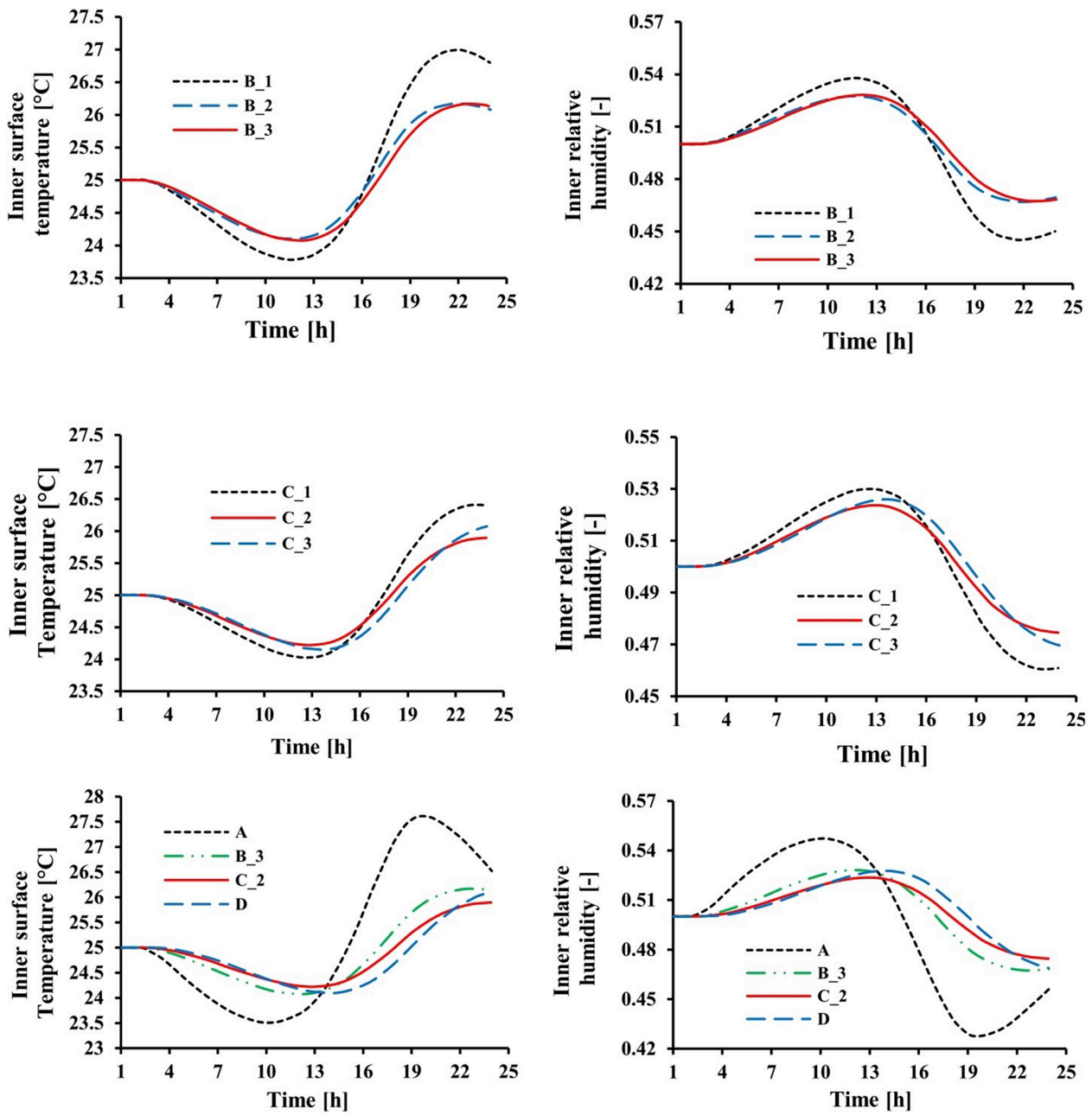


Fig. 13. Time-variation of the inner temperature, and the inner relative humidity under. Different PCHCM filling ratios, and locations in sintered hollow bricks for 24 h.

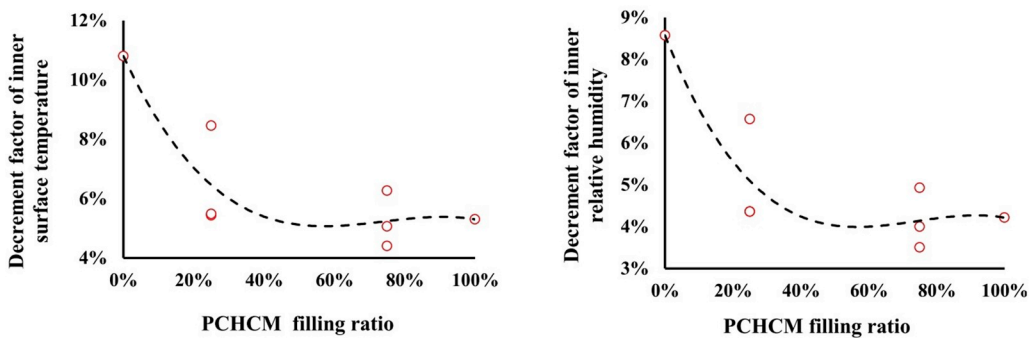


Fig. 14. Variation of the decrement factor of inner temperature, and relative humidity according to different PCHCM filling ratios and locations.

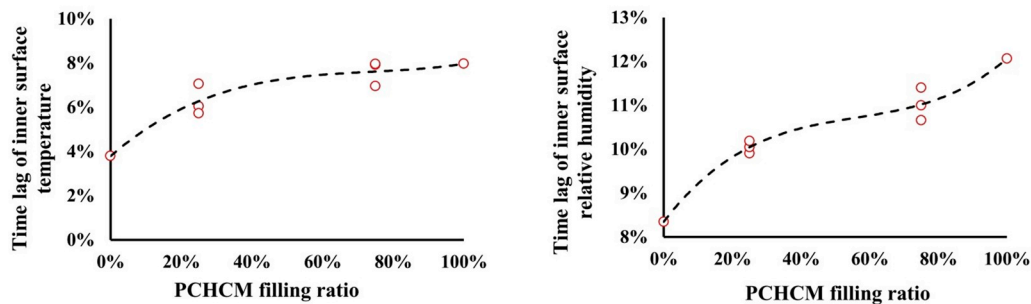


Fig. 15. Variations of the time lag of inner temperature, and relative humidity with different PCHCM filling ratios and locations.

great ability to reduce the fluctuations of inner temperature, and the relative humidity, and can reduce 50% of the total heat flux. The optimum effect of PCHCM was obtained by filling it in the center, and in the internal air cavities of the sintered hollow bricks simultaneously (case C<sub>2</sub>). With the increase of PCHCM filling ratio, the decrement factor decreases, and the time lag increases for the inner surface temperature, and relative humidity. For the same filling ratio, due to PCHCM locations, a difference of decrement factor, and time lag is observed. Above all, the proposed material (PCHCM) has the potential to be a high energy saving material, and could constitute one of the solutions for the substitution of the EPS in thermal insulating in the building.

## References

- J. Li, X. Meng, Y. Gao, W. Mao, T. Luo, L. Zhang, Effect of the insulation materials filling on the thermal performance of sintered hollow bricks, *Case stud. Therm. Eng.* 11 (2018) 62–70 <https://doi.org/10.1016/j.csite.2017.12.007>.
- A. Bouchair, Steady state theoretical model of fired clay hollow bricks for enhanced external wall thermal insulation, *Build. Environ.* 43 (2008) 1603–1618 <https://doi.org/10.1016/j.buildenv.2007.10.005>.
- Z. Chen, D. Su, M. Qin, G. Fang, Preparation and characteristics of composite phase change material (CPCM) with SiO<sub>2</sub> and diatomite as endothermal-hygroscopic material, *Energy Build.* 86 (2015) 1–6 <https://dx.doi.org/10.1016/j.enbuild.2014.10.013>.
- Z. Wu, M. Qin, Z. Chen, Phase change humidity control material and its application in buildings, *Procedia Eng.* 205 (2017) 1011–1018 <https://doi.org/10.1016/j.proeng.2017.10.162>.
- N.P. Sharifi, G.E. Freeman, A.R. Sakulich, Using COMSOL modeling to investigate the efficiency of PCMs at modifying temperature changes in cementitious materials – case study, *Constr. Build. Mater.* 101 (2015) 965–974 <https://doi.org/10.1016/j.conbuildmat.2015.10.162>.
- M. Qin, Z. Chen, Synthesis and characteristics of composite phase change humidity control materials, *Energy Procedia* 139 (2017) 493–498 <https://doi.org/10.1016/j.egypro.2017.11.243>.
- Z. Chen, M. Qin, Synthesis and characterization of composite phase change material (CPCM) with SiO<sub>2</sub> and diatomite as endothermal-hygroscopic material, *Energy Procedia* 78 (2015) 201–206 <https://doi.org/10.1016/j.egypro.2015.11.140>.
- M.Y. Ferroukhi, R. Djedjig, K. Limam, R. Belarbi, Hygrothermal behavior modeling of the hygroscopic envelopes of buildings: a dynamic co-simulation approach, *Build. Simul.* 9 (5) (2016) 501–512 <https://doi.org/10.1007/s12273-016-0292-5>.
- J.F. Nicol, M.A. Humphreys, Adaptive thermal comfort and sustainable thermal standards for buildings, *Energy Build.* 34 (2002) 563–572 [https://doi.org/10.1016/S0378-7788\(02\)00006-3](https://doi.org/10.1016/S0378-7788(02)00006-3).
- S.N. Al-Saadi, Z.J. Zhai, Modeling phase change materials embedded in building enclosure: a review, *Renew. Sustain. Energy Rev.* 21 (2013) 659–673 <https://doi.org/10.1016/j.rser.2013.01.024>.
- A. Jamekhorshid, S.M. Sadrameli, M. Farid, A review of microencapsulation methods of phase change materials (PCMs) as a thermal energy storage (TES) medium, *Renew. Sustain. Energy Rev.* 31 (2014) 531–542 <https://doi.org/10.1016/j.rser.2013.12.033>.
- A. Sharma, V.V. Tyagi, C.R. Chen, D. Buddhi, Review on thermal energy storage with phase change materials and applications, *Renew. Sustain. Energy Rev.* 13 (2009) 318–345 <https://doi.org/10.1016/j.rser.2007.10.005>.
- A. Pasupathy, R. Velraj, R.V. Seeniraj, Phase change material-based building architecture for thermal management in residential and commercial establishments, *Renew. Sustain. Energy Rev.* 12 (2008) 39–64 <https://doi.org/10.1016/j.rser.2006.05.010>.
- S.D. Zwanig, Y. Lian, E.G. Brehob, Numerical simulation of phase change material composite wallboard in a multi-layered building envelope, *Energy Convers. Manag.* 69 (2013) 27–40 <https://doi.org/10.1016/j.enconman.2013.02.003>.
- K.O. Lee, M.A. Medina, E. Raith, X. Sun, Assessing the integration of a thin phase change material (PCM) layer in a residential building wall for heat transfer reduction and management, *Appl. Energy* 137 (2015) 699–706 <https://doi.org/10.1016/j.apenergy.2014.09.003>.
- H. Xie, G. Gong, Y. Wu, Y. Liu, Y. Wang, Research on the hygroscopicity of a composite hygroscopic material and its influence on indoor thermal and humidity environment, *Appl. Sci.* 430 (8) (2018), <https://doi.org/10.3390/app8030430>.
- M. Qin, A. Ait-Mokhtar, R. Belarbi, Two-dimensional hygrothermal transfer in porous building materials, *Appl. Therm. Eng.* 30 (16) (2010) 2555–2562 <https://doi.org/10.1016/j.applthermaleng.2010.07.006>.
- D.H. Vu, K.S. Wang, B.H. Bac, B.X. Nam, Humidity control materials prepared from diatomite and volcanic ash, *Constr. Build. Mater.* 38 (2013) 1066–1072 <https://doi.org/10.1016/j.conbuildmat.2012.09.040>.
- A. Trabelsi, R. Belarbi, P. Turcry, A. Ait-Mokhtar, Water vapour desorption variability of in situ concrete and effects on drying simulations, *Mag. Concr. Res.* 63 (5) (2011) 333–342 <https://doi.org/10.1680/mac.9.00161>.
- B. Zhou, Z. Chen, Experimental study on the hygrothermal performance of zeolite-based humidity control building materials, *Int. J. Heat. Technol.* 34 (3) (2016) 407–414, <https://doi.org/10.18280/ijht.340309>.
- J. Zheng, J. Shi, Q. Ma, X. Dai, Z. Chen, Experimental study on humidity control performance of diatomite-based building materials, *Appl. Therm. Eng.* 114 (2017) 450–456 <https://doi.org/10.1016/j.applthermaleng.2016.11.203>.
- A. Bouguerra, O. Amiri, A. Ait-Mokhtar, M.B. Diop, Water sorptivity and pore structure of wood-cementitious composites, *Mag. Concr. Res.* 54 (2) (2002) 103–112 <https://doi.org/10.1680/mac.2002.54.2.103>.
- M. Tanaka, Saito, *The Variance of Humidity in Room According to Wall Materials, 3rd version*, Shukosha Printing Co., Ltd., Fukuoka, 1949, pp. 21–25 *Research Report of Architectural Institute of Japan*.
- T. Horikawa, Y. Kitakaze, T. Sekida, J.I. Hayashi, M. Katoh, Characteristics and humidity control capacity of activated carbon from bamboo, *Bioresour. Technol.* 101 (11) (2010) 3964–3969 <https://doi.org/10.1016/j.biortech.2010.01.032>.
- T. Hasegawa, S. Iwasaki, Y. Shibutani, I. Abe, Preparation of superior humidity-control materials from kenaf, *J. Porous Mater.* 16 (2) (2009) 129–134 <https://doi.org/10.1007/s10934-007-9176-5>.
- J.J.D.C. Díaz, F.P.A. Rabanal, P.J.G. Nieto, J.D. Hernandez, B.R. Soria, J.M. Pérez-Bella, Hygrothermal properties of lightweight concrete: experiments and numerical fitting study, *Constr. Build. Mater.* 40 (2013) 543–555 <https://doi.org/10.1016/j.conbuildmat.2012.11.045>.
- R.M. Wang, J.F. Wang, X.W. Wang, Y.F. He, Y.F. Zhu, M.L. Jiang, Preparation of acrylate-based copolymer emulsion and its humidity controlling mechanism in interior wall coatings, *Prog. Org. Coating* 71 (4) (2011) 369–375 <https://doi.org/10.1016/j.porgcoat.2011.04.007>.
- L. Navarro, A. de Gracia, S. Colclough, M. Browne, S.J. Mc-Cormack, P. Griffiths, L.F. Cabeza, Thermal energy storage in building integrated thermal systems: a review. Part 1. Active storage systems, *Renew. Energy* 88 (2016) 526–547 <https://doi.org/10.1016/j.renene.2015.11.040>.
- F. Bruno, M. Liu, N.H.Z. Tay, Using solid-liquid phase change materials (PCMs) in thermal energy storage systems, *Advances in Thermal Energy Storage Systems (Methods and Applications)*, Woodhead Publishing Series in Energy, 2015, pp. 201–246 <https://doi.org/10.1016/C2013-0-16453-7>.
- Y. Yuan, H. Zhang, N. Zhang, Q. Sun, X. Cao, Effect of water content on the phase transition temperature, latent heat and water uptake of PEG polymers acting as endothermal hygroscopic materials, *J. Therm. Anal. Calorim.* 126 (2) (2016) 699–708 <https://doi.org/10.1007/s10973-016-5537-0>.
- S. Karaman, A. Karaipekli, A. Sari, A. Biçer, Polyethylene glycol (PEG)/diatomite composite as a novel form-stable phase change material for thermal energy storage, *Sol. Energy Mater. Sol. Cells* 95 (2011) 1647–1653 <https://doi.org/10.1016/j.solmat.2011.01.022>.
- J.L. Shang, Z.F. Zong, H. Zhang, Synthesis and analysis of new humidity-controlling composite materials, *Int. J. Min. Metall. Mater.* 24 (5) (2017) 594 <https://doi.org/10.1007/s12613-017-1441-2>.
- UNEP-POPS-NIP-GUID-InventoryAndSubstitution-HBCD-201703.En, Guidance for Inventory and Substitution.Pdf.
- H. Meradi, L.H. Atoui, L. Bahloul, K. Labiod, F. Ismail, Characterization of diatomite from Sig region (West Algeria) for industrial application, *Manag. Environ. Qual. Int. J.* 27 (3) (2016) 281–288 <https://doi.org/10.1108/MEQ-04-2015-0057>.
- B. Hamdi, S. Hamdi, Thermal properties of Algerian diatomite, study of the possibility to its use in the thermal insulation, *Springer Proc. Phys.* 155 (2014) 27–32 [https://doi.org/10.1007/978-3-319-05521-3\\_4](https://doi.org/10.1007/978-3-319-05521-3_4).
- F. Tariku, K. Kumaran, P. Fazio, Transient model for coupled heat, air and moisture transfer through multilayered porous media, *Int. J. Heat Mass Transf.* 53 (2010) 3035–3044 <https://doi.org/10.1016/j.ijheatmasstransfer.2010.03.024>.
- H.M. Kunzel, *Simultaneous Heat and Moisture Transport in Building Components. One- and Two Dimensional Calculation Using Simple Parameters*, Dissertation university Stuttgart, Germany, 1995 (ISBN 3-8167-4103-7).
- A.I.N. Korti, Numerical heat flux simulations on double-pass solar collector with

- PCM spheres media, *International Journal of Air-Conditioning and Refrigeration* 24 (2) (2016) 13 <https://doi.org/10.1142/S2010132516500103>.
- [39] R.J. De-Dear, E. Arens, Z. Hui, Convective and radiative heat transfer coefficients for individual human body segments, *Int. J. Biometeorol.* 40 (1997) 141–156 <https://doi.org/10.1007/s004840050035>.
- [40] C.E. Hagentoft, A.S. Kalagasidis, B. Adl-Zarrabi, Assessment method of numerical prediction models for combined heat, air and moisture transfer in building components: benchmarks for one-dimensional cases, *J. Therm. Envelope Build. Sci.* 27 (4) (2004) 327–352 <https://doi.org/10.1177/1097196304042436>.
- [41] F. Liu, B. Jia, B. Chen, Influence of hygroscopic material on indoors environment, *Procedia Eng.* 205 (2017) 3662–3669 <https://doi.org/10.1016/j.proeng.2017.10.240>.
- [42] A.G. FEMLAB, Comsol 33 Multiphysics FEM Software Package, (2007).
- [43] <https://www.infoclimat.fr/climatologie-mensuelle/60531/aout/2017/temperatures.html>.
- [44] Fraunhofer WUFI Light 6.2.1 free version, Germany: Fraunhofer IBP, Available from: <https://wufi.de/en/webshop/>.
- [45] H. Asan, Numerical computation of time lags and decrement factors for different building materials, *Build. Environ.* 41 (2006) 615–620 <https://doi.org/10.1016/j.buildenv.2005.02.020>.
- [46] N. Degirmenci, A. Yilmaz, Use of diatomite as partial replacement for Portland cement in cement mortars, *Constr. Build. Mater.* 23 (2009) 284–288 <https://doi.org/10.1016/j.conbuildmat.2007.12.008>.